International Journal of Marine Engineering Innovation and Research, Vol. 9(1), March. 2024. 47-57
(pISSN: 2541-5972, eISSN: 2548-1479)

Performance Improvement Incremental Conductance Algorithm using Incremental Fuzzy to Reach GMPP under Partial Shading Conditions

Imam Sutrisno [1], Joessianto Eko Poetro [2], Pranowo Sidi [3], Boedi Herijono [4], Antonius Edy Kristiyono [5], Monika Retno Gunarti [6]

(Received: 5 March 2024 / Revised: 10 March 2024 /Accepted: 9 March 2024)

***Abstract*↓ This paper proposes an improved Maximum Power Point Tracking (MPPT) algorithm for photovoltaic (PV) systems under partial shading conditions. The proposed method enhances the widely used Incremental Conductance (IC) algorithm by incorporating an incremental fuzzy control technique. The conventional IC algorithm suffers from limitations in adapting to rapidly changing irradiation conditions due to its fixed step size. The proposed Inc-Fuzzy algorithm dynamically adjusts the step size based on the change in power and voltage, enabling it to better track the Global Maximum Power Point (GMPP) under partial shading. Simulation results demonstrate that the Inc-Fuzzy algorithm achieves an average accuracy of 98.29% under constant irradiation and outperforms the conventional IC algorithm by 1.69% in terms of captured power during sudden irradiation changes. This improvement highlights the effectiveness of the Inc-Fuzzy approach in enhancing the performance of MPPT for PV systems under challenging operating conditions.**

Keywords – Fuzzy Control, Incremental Conductance, Partial Shading, MPPT Optimization, GMPP Tracking, Photovoltaic Systems, Step Size Adjustment, Dynamic Adaptation, Power Electronics, Irradiation Changes

I. INTRODUCTION

Solar panels convert sunlight into electricity, offering a clean and sustainable energy source. This generated electricity can be stored in batteries for nighttime use, powering lights and appliances, or used directly without battery storage. However, the output of solar panels isn't constant; it varies based on factors like temperature, sunlight intensity (irradiation), and the electrical load placed on the system. Additionally, the electrical power generation depends on the specific characteristics of the solar panels themselves, like their short circuit current (Isc) and open-circuit voltage (Voc) [1]. Controlling the voltage of solar cells allows us to extract the maximum power they can generate under specific conditions.

Solar panels have the potential to generate significant amounts of electricity. However, their efficiency can fluctuate due to changing weather conditions, especially variations in sunlight intensity (irradiation) [2]. To address this issue, a technique called Maximum Power Point Tracking (MPPT) is employed. MPPT works by continuously adjusting the voltage of the solar panels to reach the Maximum Power Point (MPP). This MPP is the point where the panels produce their highest power output under specific conditions. One common MPPT method, the Incremental Conductance (IC) algorithm, analyzes changes in the solar panel's conductance to track the MPP. While this method performs well under various weather conditions, it has a critical limitation. The IC algorithm relies on a set "step size" for voltage adjustments. This step size can be problematic: Large step size: If the step size is too large, the system can experience oscillations around the MPP, leading to wasted power. Small step size: Conversely, a very small step size slows down the tracking process, potentially missing the MPP during rapid changes in irradiation. Finding the perfect balance between accuracy and tracking speed by adjusting the step size is a challenge [3]. This paper proposes a modified version of the IC algorithm that incorporates Fuzzy Logic Control (FLC) to overcome this limitation. Fuzzy logic is an intelligent control technique that can handle complex systems like solar panels and make adjustments dynamically based on the operating conditions. By incorporating fuzzy logic, the proposed method aims to automatically adjust the step size based on the severity of the error from the MPP, leading to faster and more accurate tracking even under fluctuating irradiation.

Numerous Maximum Power Point Tracking (MPPT) methods have been developed to enhance the efficiency of solar panels. One widely used approach is the Incremental Conductance (IC) algorithm. Studies have demonstrated that the IC method effectively increases the output power of solar panels [4, 5]. In one application, the IC algorithm was implemented on a switching SEPIC

Imam Sutrisno is with Politeknik Perkapalan Negeri Surabaya, Indonesia. E-mail:imams3jpg@yahoo.com
Joessianto Eko Poetro is with Politeknik Perkapalan Negeri Surabaya, Indonesia. E-mail joessianto@yahoo.com
Pranowo Sidi is with Politeknik Perkapalan Negeri Surabaya, Indonesia. E-mail: pransidi@ppns.ac.id
Boedi Herijono is with Politeknik Perkapalan Negeri Surabaya, Indonesia. E-mail: boediherijono@yahoo.co.id
Antonius Edy Kristiyono is with Politeknik Pelayaran Surabaya, Indonesia. E-mail: edyantonius25@gmail.com
Monika Retno Gunarti is with Politeknik Pelayaran Surabaya, Indonesia. E-mail: monikaretnogunarti33@gmail.com

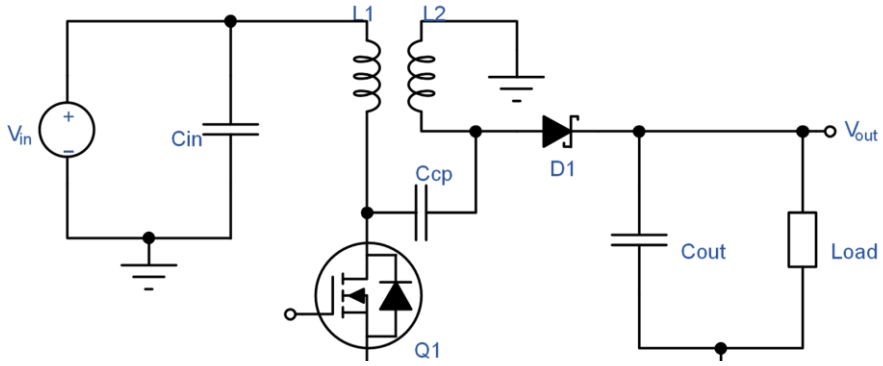

Figure. 1. Sepic Converter Circuit.

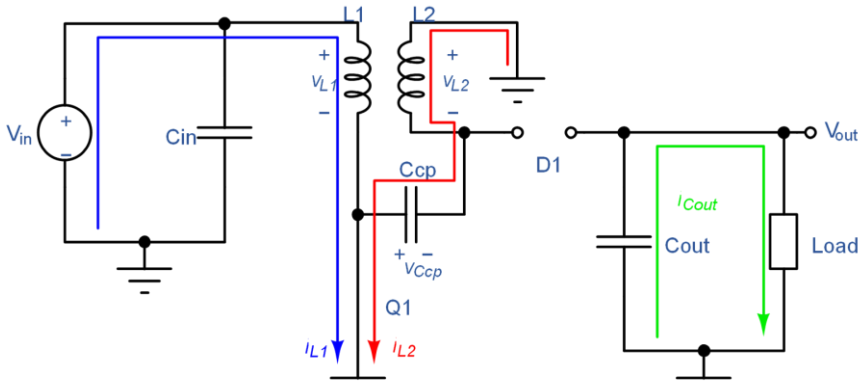

Figure. 2. Sepic converter circuit when switch Q1 is ON

converter using a Pulse Width Modulation (PWM) wave generated by an Arduino microcontroller at a frequency of 62.5 kHz to adjust the voltage based on a setpoint [6].

Comparative analyses of various conventional MPPT methods have been conducted by researchers ([7], [8], [9]). These studies concluded that incorporating a variable step size into the IC method offers the most effective solution for finding the maximum power point. However, the IC algorithm has its drawbacks. To address these limitations, a variable step-size modification technique has been proposed [10, 11, 12]. This technique utilizes a scaling factor heavily reliant on the voltage change of the photovoltaic (PV) module. The proposed technique has shown improvements in both steady-state and dynamic performance responses.

Research on artificial intelligence-based methods for MPPT suggests advantages such as faster tracking and better environmental condition correction [13, 14]. However, these methods also come with drawbacks, including more complex implementation and higher costs. The use of fuzzy logic, a type of artificial intelligence, offers benefits like faster tracking and reduced power oscillations [15, 16, 17]. In contrast, the Particle Swarm Optimization (PSO) algorithm demonstrates advantages in achieving a better maximum power point under partial shading conditions [18, 19, 20]. Studies have investigated the behavior of MPPT trackers modeled using IC algorithms under rapidly changing environmental conditions such as temperature and irradiation levels [21]. The fixed step size employed by the IC alg oscillations orithm leads to during steady-state operation. Research by [22] proposes a novel approach based on fuzzy logic that can guarantee improved performance. The investigated system used to validate the proposed method consisted of a Kaneka K60 photovoltaic panel connected to a resistively loaded SEPIC converter. All results cited in this work were obtained using MATLAB-Simulink software.

Building upon these advancements, [23] proposes a revised additional conductance method combined with a Fuzzy Logic Controller (FLC) to enhance the conversion system's efficiency and operability under practical conditions. This research specifically focuses on reducing power oscillations during

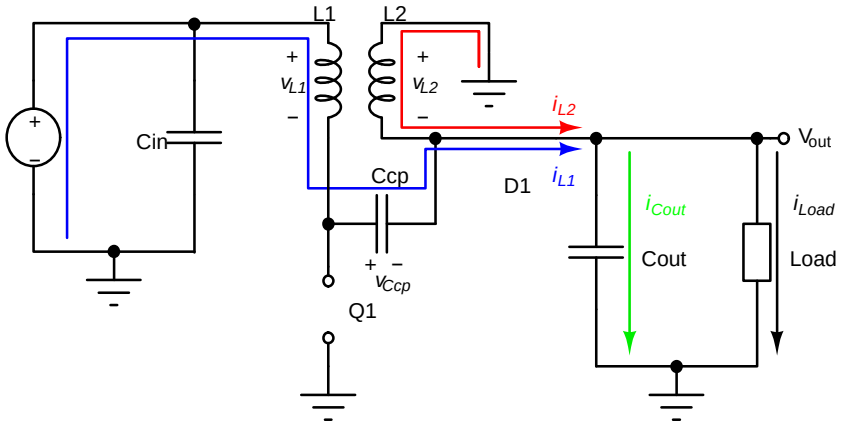

Figure. 3. Sepic Converter circuit when switch Q1 is Off.

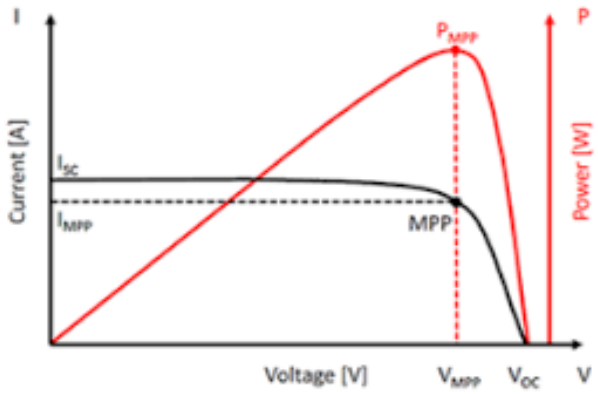

Figure. 4. Photovoltaic Characteristic Curve

rapid climate changes by integrating two Sugeno fuzzy processes with the Incremental Conductance algorithm.

II. METHOD

A. Design of Sepic Converter

The SEPIC converter, a type of DC-DC converter, is known for its ability to produce an output voltage that can be greater than, smaller than, or equal to the input voltage [24]. This flexibility makes it a valuable tool in various applications. The SEPIC converter consists of two main types of components:

Active components: These are semiconductor devices capable of switching, such as Metal-Oxide-Semiconductor Field-Effect Transistors. They play a crucial role in directing the flow of current within the circuit. Passive components: These include diodes, inductors, capacitors, and load resistors. They contribute to filtering, energy storage, and voltage regulation within the system. Due to the presence of switching elements, the SEPIC converter can be classified as a second-order system. Additionally, its output voltage exhibits nonlinear behavior over time, primarily due to the switching operation. Visualizing the SEPIC Converter (Figure 1): For a clearer understanding, Figure 1 presents a schematic diagram of the SEPIC converter circuit, illustrating the arrangement and connections of the various components mentioned above. As the SEPIC converter is a second-order system, analyzing its behavior under different operating conditions requires determining several crucial parameters. These parameters hold significant importance in understanding and predicting the converter's output characteristics.

$$\Delta I_L = IL_{max} - IL_{min} \quad (1)$$

$$D = \frac{T_{on}}{T} = \frac{T_{on}}{T_{on}+T_{off}} \quad (2)$$

$$\Delta t_{on} = T_{on} = DT_{sw} \quad (3)$$

$$\Delta t_{off} = T_{off} = T - DT_{sw} = (1-D)T_{sw} = D'T_{sw} \quad (4)$$

During the period when switch Q1 is turned on: Inductor L1: This component acts as the primary energy source, receiving current directly from the input voltage source (Vin) and storing energy within its magnetic field. Inductor L2: While Q1 is on, L2 receives energy from the coupling capacitor (Ccp). The direction of current flow

through L2 is reversed compared to its state when Q1 is off.

Diode D1: In this state, D1 becomes reverse biased, effectively blocking any current flow through it. The Cout capacitor plays a crucial role in supplying current to the load during this on state. Figure 2 provides an equivalent circuit diagram for the SEPIC converter when switch Q1 is turned on. This simplified diagram helps visualize the energy flow and interactions between components in this operating mode. Based on the analysis of Figure 2, the following adjustments can be identified as follows:

$$V_{L1} = V_S \quad (5)$$

$$V_{L2} = V_{Ccp} \quad (6)$$

$$i_{Ccp} = -i_{L2} \quad (7)$$

$$i_{Cout} = \frac{-V_{Cout}}{R\ Load} \quad (8)$$

When switch Q1 is turned off: Diode D1: This component becomes forward biased, allowing current to flow through it. As a result, inductor L1 transfers the energy it stored during the on state to the coupling capacitor (Ccp). Inductors L1 and L2: Both inductors contribute to supplying current to the output capacitor (Cout) and the load resistor (R Load) in this off state. The direction of current flow through L1 is reversed compared to its state when Q1 is on. L2 maintains its current direction from the on state. Equivalent Circuit: Figure 3 depicts the equivalent circuit of the SEPIC converter during this off state, highlighting the changes in component behavior and energy flow compared to the on state. Analyzing Figure 3 reveals the following ad

$$V_{L1} = V_S - V_{Ccp} - V_{Cout} - V_D \quad (9)$$

$$V_{L2} = -V_{Cout} - V_D \quad (10)$$

$$i_{Ccp} = i_{L1} \quad (11)$$

$$i_{Cout} = i_{L1} + i_{L2} - \frac{V_{Cout}}{R\ Load} \quad (12)$$

The duty cycle, a crucial parameter in SEPIC converters, can be calculated by applying the principle of Volt-Second Balance to both inductors, L1 and L2. Equations 5 and 6, which are not provided here, represent the mathematical expressions for this balance applied to each inductor, respectively. By solving these equations along with other relevant circuit parameters, the duty cycle of the SEPIC converter can be obtained.

$$< V_{L1} >_{Tsw} = \frac{1}{T_{sw}}\left[\int_0^{DT_{sw}} V_S\ dt + \int_{DT_{sw}}^{T_{sw}} V_S - V_{Ccp} - V_{Cout} - V_D\ dt\right] = 0$$

$$= \frac{1}{T_{sw}}\left[V_S\ (DT_{sw}) + (V_S - V_{Ccp} - V_{Cout} - V_D)(T_{sw} - DT_{sw}\right]$$

$$= 0$$

$$= DV_S + D'(V_S - V_{Ccp} - V_{Cout} - V_D)$$

$$= DV_S - D'V_{Ccp} - D'V_{Cout} - D'V_D = 0 \quad (13)$$

$$< V_{L2} >_{Tsw} = \frac{1}{T_{sw}}\left[\int_0^{DT_{sw}} V_{Ccp}\ dt + \int_{DT_{sw}}^{T_{sw}} -V_{Cout} - V_D\ dt\right] = 0$$

$$= \frac{1}{T_{sw}}\left[V_{Ccp}\ (DT_{sw}) - (V_{Cout} + V_D)(T_{sw} - DT_{sw}\right] = 0$$

$$= DV_{Ccp} - D'V_{Cout} - D'V_D = 0 \quad (14)$$

Upon subtracting equation 5 from equation 6, we obtain :

$$V_{Ccp} = V_S \quad (15)$$

Substituting the value of equation 15 into equation 14 leads to the formula for the duty cycle of a SEPIC converter, as shown below:

$$DV_{Ccp} - D'V_{Cout} - D'V_D = 0$$

$$D(V_S) = D'(V_{Cout} + V_D)$$

$$V_{Cout} + V_D = \frac{D}{D'}V_S = \frac{D}{1-D}V_S \quad (16)$$

$$D = \frac{V_{Cout} + V_D}{V_S + V_{Cout} + V_D} \quad (17)$$

TABLE 1.
SEPIC CONVERTER SPECIFICATION

Characteristics	Nominal
Vin	8 V - 21,8 V
Vout	14,4 V – 20 V
Maximum Iout	5 A
Switching Frequency	40 kHz
Maximum current ripple	20 %
Voltage Ripple	0,5 %

B. Design of Incremental Conductance – Fuzzy Logic Controller

The Incremental Conductance algorithm finds the point on the solar cell's power-voltage curve where the slope is zero. This point corresponds to the maximum power output of the solar cell. It works by comparing the change in power with the change in voltage, which is the slope of the power-voltage curve. When the slope is zero, the change in power is zero, and the solar cell is operating at its maximum power point. The Incremental Conductance (InC) algorithm tracks the maximum power output of a solar cell. It does this by measuring changes in the cell's conductance, which relates its current and voltage. This allows the algorithm to understand how power changes with fluctuations in the current (Ipv) caused by varying irradiation levels. Based on the measured conductance, the algorithm determines the reference voltage (Vref) that needs to be applied to reach the state where: dI/dV + I/V

= 0 [25]. This equation represents the point on the power-voltage curve where the slope is zero, corresponding to the maximum power output. Figure 4 illustrates the three different operating conditions the InC algorithm encounters, categorized based on the sign of that equation. To improve the performance of the Incremental Conductance (InC) algorithm, a fuzzy logic controller is introduced. This controller allows for finer adjustments to the step size (Dstep) based on the magnitude of the error between the actual power change and the desired power change caused by variations in solar panel voltage. The fuzzy logic controller utilizes the photovoltaic characteristic curve (Figure 5) as a reference to define its membership functions and fuzzy rules. This curve represents the relationship between voltage, current, and power output of the solar panel. The slope of the power-voltage curve and the current-voltage curve are divided into five zones. These zones represent different magnitudes of the error value and the change in current (delta I). The fuzzy logic controller uses this information to determine the appropriate adjustments to Dstep [26].

The fuzzy logic controller operates by dividing the operating space into five zones (A-E) based on the magnitude and sign of both the error value (difference between desired and actual power change) and the change in current (delta I). Zone A: When both error and delta I are positively large, the controller significantly increases the step size (Dstep) to achieve a large increase in the reference voltage (Vref). This accelerates the movement towards the maximum power point. Zone B: When both error and delta I are positively small, the controller minimally increases Dstep, resulting in a small increase in Vref. This fine-tunes the voltage change for precise movement. Zone C: When both error and delta I are zero, the controller maintains the current Dstep value, indicating the system is already at the optimal operating point. Zone D: When both error and delta I are negatively small, the controller minimally decreases Dstep, resulting in a small decrease in Vref. This carefully adjusts the voltage to prevent overshooting the maximum power point. Zone E: When both error and delta I are negatively large, the controller significantly decreases Dstep, causing

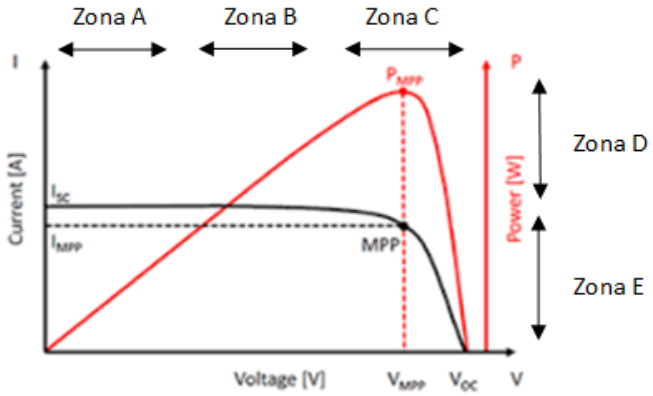

Figure. 5. Photovoltaic Performance Curve Zone Division

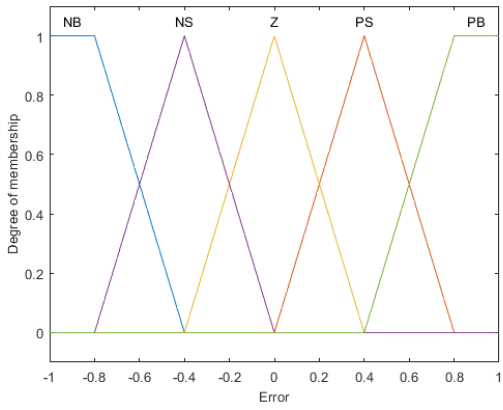

Figure. 6. Membership Function of Input Error

a large decrease in Vref [27]. This helps the system move away from a suboptimal operating point and towards the maximum power point.

The fuzzy logic controller in this case utilizes the Takagi-Sugeno (TS) approach. This is a type of fuzzy system that outputs crisp (non-fuzzy) values based on fuzzy inputs. The two TS fuzzy controllers are embedded within the five distinct categories: Positive Big, Positive Small, Zero, Negative Big, and Negative Small. Consistent with the chosen Takagi-Sugeno (TS) fuzzy approach, the Dstep values in each category are represented using fixed, predefined values instead of fuzzy sets. This characteristic is unique to TS fuzzy systems. Figure 7 specifically illustrates the membership function for the Dstep1 output

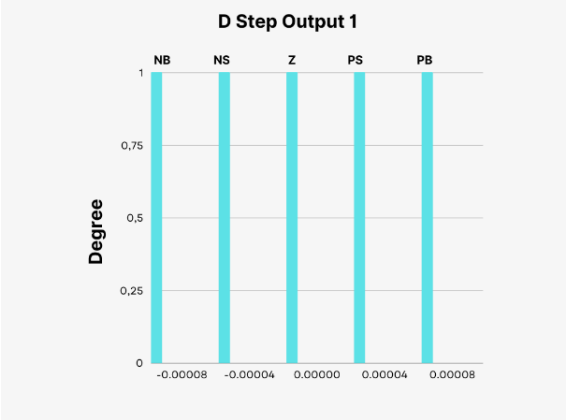

Figure. 7. Membership Function Output DStep 1

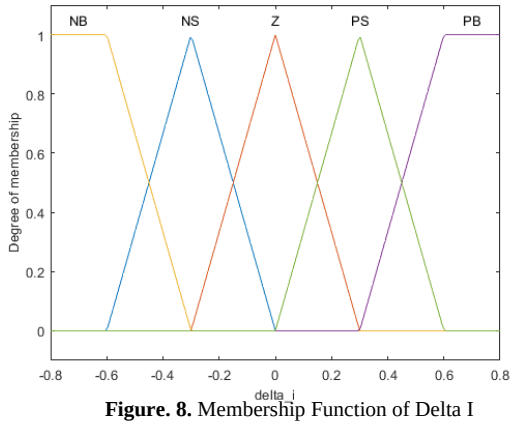

Figure. 8. Membership Function of Delta I

basic Inc algorithm, preserving its core functionality. The first fuzzy set uses the error value as input (SISO type), while the second uses the change in current (delta I) (also

category, providing further insight into the fuzzy logic controller's behavior. This section introduces the rule base for the first fuzzy set within the fuzzy logic controller.

TABLE 2.
RULE BASE OF FUZZY SET 1

R	Input Error	Output Dstep1
1	Negatif Big	Positif Big
2	Negatif Small	Positif Small
3	Zero	Zero
4	Positif Small	Negatif Small
5	Positif Big	Negatif Big

SISO type). These fuzzy outputs influence the step size adjustment, ultimately leading to finer control of the reference voltage and faster convergence to the maximum power point. Similar to the error and delta I, the output for Dstep, which controls the voltage adjustments, also has

This set specifically deals with the error value, which represents the difference between desired and actual power change.

Table 2 visually presents the established fuzzy rules for this set. These rules define how the controller should

adjust the step size (Dstep) based on the magnitude and sign of the error value (positive or negative, large or small) detected in the system. This fuzzy set becomes active only when the voltage difference (dV) reaches zero. When active, it utilizes a membership function named "Delta I" or "Flow Change". This function employs five linguistic variables to represent different ranges of values: Negative Big (NB), Negative Small (NS), Zero (Z), Positive Small (PS), Positive Big (PB). The values associated with these linguistic variables range from -0.8 to +0.8, as depicted in Figure 8. This figure likely presents the graphical representation of the membership function for Delta I. The output from Fuzzy Step 2 shares the same range as the output from Fuzzy Step 1. This is because both sets ultimately influence the same control variable - the Duty Cycle within the SEPIC converter circuit. This section introduces the rule base for the second fuzzy set. This set focuses on the change in current (Delta I), also referred to as "Flow Change". Table 3 visually presents

TABLE 3.
RULE BASE OF FUZZY SET 2

R	Input Delta I	Output Dstep2
1	Negatif Big	Positif Big
2	Negatif Small	Positif Small
3	Zero	Zero
4	Positif Small	Negatif Small
5	Positif Big	Negatif Big

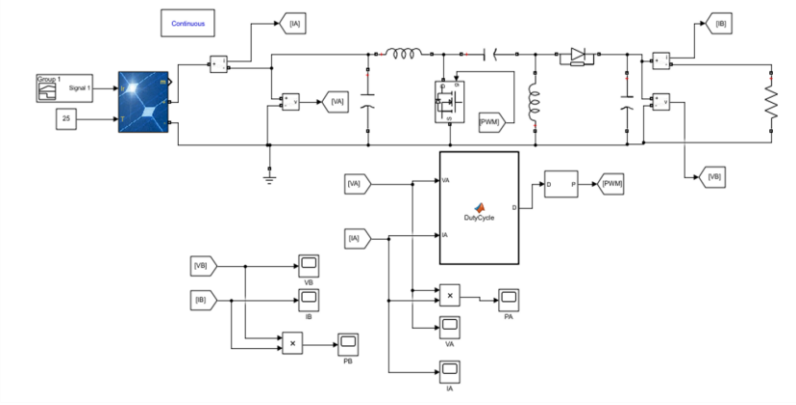

Figure. 9. Inc-Fuzzy Algorithm Test Circuit

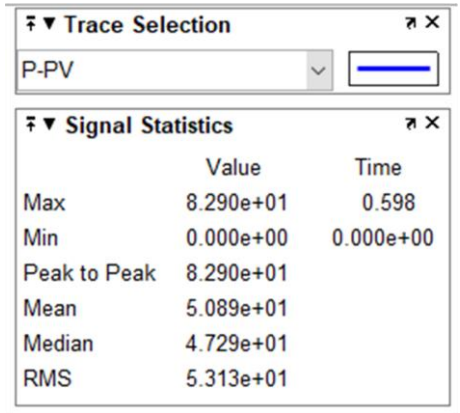

Figure. 10. Graph of Power, Voltage and Current at 800 W/m^2 Irradiation

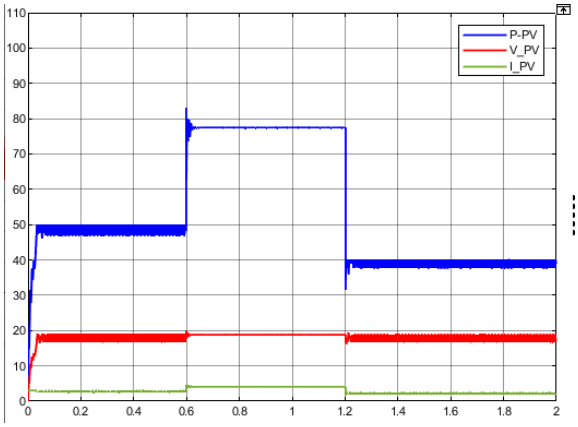

Figure. 11. Graph of Power Tracking Incremental Conductance Algorithm on Irradiation Changes.

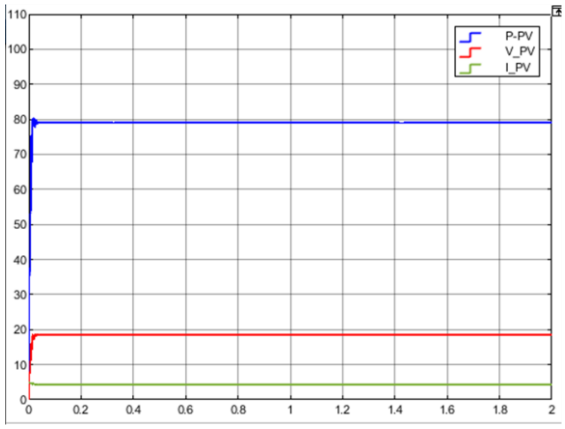

Figure. 12. Statistics of Power Tracking Algorithm Incremental Conductance

TABLE 4.
INC-FUZZY ALGORITHM TRACKING RESULTS ON CONSTANT IRRADIATION

Irradiation(W/m^2)	Vpv(V)	Ipv(A)	Vout(V)	Iout(A)	Ppv(W)	Pout(W)	Pmax Theory(W)	Accuracy (%)	Eff (%)
100	16,37	0,57	15,47	0,509	9,33	7,87	9,62	96,95	84,38
200	17,39	1,118	16,37	1,054	19,402	17,25	19,72	98,55	88,74
300	17,83	1,657	16,7	1,593	29,541	26,6	29,91	98,76	90,04
400	18,08	2,189	16,85	2,124	39,572	35,78	40,09	98,7	90,42
500	18,22	2,721	16,88	2,657	49,576	44,85	50,23	98,68	90,46
600	18,33	3,243	16,88	3,179	59,44	53,66	60,31	98,55	90,27
700	18,39	3,762	16,84	3,699	69,18	62,29	70,3	98,4	90,03
800	18,44	4,272	16,78	4,211	78,77	70,66	80,2	98,21	89,69
900	18,39	4,817	16,62	4,758	88,58	79,07	89,97	98,45	89,26
1000	18,45	5,293	16,58	5,235	97,65	86,79	99,99	97,66	88,87

the established fuzzy rules for this set. These rules define how the controller should adjust the step size (Dstep) based on the magnitude and sign of the Delta I value (positive or negative, large or small) detected in the system.

III. RESULTS AND DISCUSSION

The MPPT (Maximum Power Point Tracking) algorithm, combining Incremental Conductance (InC) and fuzzy logic (Fuzzy), is tested using MATLAB 2019 software. A function block programmed in C simulates

the microcontroller responsible for controlling the MPPT algorithm. This block acts as the brain of the system. The test setup incorporates a model of a photovoltaic (PV) array that reflects real-world conditions. This model allows for adjustments in both irradiation levels and temperature, mimicking various environmental scenarios. Additionally, the electrical parameters of the PV model can be tailored to match specific PV specifications. The chosen PV module is a monocrystalline type with a maximum power output of 100 Watts, operating at a voltage of 17.8 Volts (Vmp) and a current of 5.62 Amps (Imp) under peak conditions.

The MPPT InC-Fuzzy algorithm is evaluated under two different conditions: Constant Irradiation: This test assesses the algorithm's performance under stable lighting conditions. Rapid Irradiation Change: This test simulates a sudden change in light levels, evaluating the algorithm's ability to adapt and maintain optimal power output. A previously designed SEPIC converter circuit is used to interface the MPPT algorithm with the PV array and adjust the system's voltage and current levels. Figure 9 provides a schematic diagram of the test circuit for the InC-Fuzzy algorithm, offering a visual representation of the setup.

A. MPPT Testing at Constant Irradiation

This section describes the testing procedure for the MPPT algorithm under constant light conditions. A signal generator is used to provide varying irradiance levels as input to the PV block. The test covers a range of irradiance values, starting from 100 W/m² up to 1000 W/m². The test is conducted at a constant temperature of 25°C. Each test run lasts for 2 seconds. The SEPIC converter's load is

TABLE 5.
RESULTS OF TRACKING ALGORITHM INC ON IRRADIATION CHANGE

Time (s)	Ipv (A)	Vpv (V)	Vout (V)	dv (V)	di (A)	di/dv	Neg I/V	D(k-1)
0	0	0	0	0	0	0	0	0
0,1	2,64	18,55	12,75	18,55	2,64	0,1423	-0,1423	0,40734
0,2	2,48	18,96	12,25	0,41	-0,16	-0,390	-0,1308	0,39250
0,3	2,77	18,01	13,06	-0,95	0,29	-0,305	-0,1538	0,42034
0,4	2,89	16,88	14,14	-1,13	0,12	-0,10	-0,1712	0,45583
0,5	2,88	17,04	14,15	0,16	-0,01	-0,062	-0,1690	0,45367
0,6	4,57	18,16	13,13	1,12	1,69	1,5089	-0,2516	0,41962
0,7	4,25	18,54	16,92	0,38	-0,32	-0,842	-0,2292	0,47715
0,8	4,25	18,54	16,92	0	0	~	-0,2292	0,47715
0,9	4,25	18,54	16,92	0	0	~	-0,2292	0,47715
1	4,25	18,54	16,92	0	0	~	-0,2292	0,47715
1,1	4,25	18,54	16,91	0	0	~	-0,2292	0,47700
1,2	4,25	18,55	16,9	0,01	0	0	-0,2291	0,47672
1,3	2,33	16,76	12,94	-1,79	-1,92	1,0726	-0,1390	0,43569
1,4	2,2	18,11	11,4	1,35	-0,13	-0,096	-0,1214	0,38630
1,5	2,05	18,74	11,06	0,63	-0,15	-0,238	-0,1093	0,37114
1,6	2,31	17,15	12,71	-1,59	0,26	-0,163	-0,1346	0,42565
1,7	2,3	17,18	12,34	0,03	-0,01	-0,333	-0,1338	0,41802
1,8	2,02	18,83	10,8	1,65	-0,28	-0,169	-0,1072	0,36449
1,9	2,22	17,99	11,91	-0,84	0,2	-0,238	-0,1234	0,39832
2	2,33	16,76	12,93	-1,23	0,11	-0,089	-0,1390	0,43550

adjusted to an optimal resistor for each specific irradiance level. This optimal resistance value is calculated by dividing the PV's voltage at peak power (Vmp) by its current at peak power (Imp). The MPPT algorithm starts with an initial duty cycle (Dinit) of 40% (0.4). Figure 10 showcases a graph depicting power, current, and voltage at an irradiance level of 500 W/m². Table 4 likely contains a comprehensive overview of the tracking data obtained across all tested irradiance levels. The table includes a column named "Pmax Theory," which represents the theoretical maximum power output of the 100 Wp solar panels at different irradiance levels. This data serves as a benchmark to assess the accuracy of the MPPT (Maximum Power Point Tracking) algorithm's performance. A higher Ppv (actual power generated by the solar panel) value closer to the corresponding "Pmax Theory" value indicates better accuracy. The results presented in the table demonstrate that the InC-Fuzzy MPPT algorithm performs well under constant irradiation conditions. This is evident from the average accuracy of 98.291% and the average efficiency of 89.21%. These values suggest that the algorithm effectively tracks the maximum power point of the solar panel under steady lighting conditions.

B. Testing the Incremental Conductance Algorithm on Variable Irradiation

The next test is conditioned to determine the performance of MPPT Inc-Fuzzy if there is a rapid and sudden increase or decrease in irradiation. With a load resistor of 4 Ohm, the amount of irradiation was changed from 500 W/m^2 to 800W/m^2 at 0.6 seconds and then reduced to 400W/m^2 at 1.2 seconds. The tracking process of the Inc-Fuzzy Algortima that has been designed is compared with the basic Incremental Conductance Algorithm with a fixed Dstep of 6.10^{-5}. The results of tracking power, large currents and voltages from the basic algorithm of Incremental Conductance can be seen in Figure 11. The IC algorithm tracks the maximum power accurately, though steady-state oscillations are present. Oscillations are larger at lower irradiation levels (500 and 400 W/m²) compared to the smaller oscillations at 800 W/m². This is likely because the 4-ohm load is optimal at 800 W/m². These oscillations lead to suboptimal power generation, with a total root-mean-square (RMS) power loss of 53.13 watts within 2 seconds. Refer to Table 5 for easier interpretation of the tracking results. The table can also verify the IC algorithm's functionality by comparing the increment value (ΔG) and the current conductance (G(k)) to generate the output D(k-1). This value, in turn, determines the voltage (Vpv) and current (Ipv) in the next iteration. In simpler terms, while the IC algorithm tracks the maximum power well, it suffers from oscillations at specific points, impacting overall power generation efficiency. Table 5 provides additional details for further analysis. The duty cycle adjusts by a fixed increment (Dstep) of 6.10^-5, but over 0.1-second intervals, these adjustments can accumulate, resulting in larger increases or decreases in multiples of Dstep. When irradiation remains constant, the algorithm aims to maintain a specific condition (di/dv = -I/V) to reach the maximum power point. This information is also presented in Table 5: if the change in conductance (ΔG) is greater than the current conductance (G(k)), the duty cycle decreases to increase the reference voltage (Vref). Conversely, if ΔG is smaller than G(k), the duty cycle increases to reduce Vref. At 0.6 seconds, the significant increase in the duty cycle responds to the higher irradiation. As the irradiation rises, so does the power generated by the photovoltaic (PV) system. Therefore, the algorithm prioritizes current by increasing the duty cycle for optimal power production. On the other hand, the duty cycle decreases sharply at 1.2 seconds due to the decreased irradiation. With lower irradiation, the PV output is reduced, prompting the algorithm to lower the duty cycle to optimize voltage with a smaller current.

IV. CONCLUSION

The InC-Fuzzy algorithm achieves an average accuracy of 98.29% when the irradiation level remains constant. This indicates that the algorithm effectively tracks the maximum power point under stable conditions. When the irradiation level undergoes a sudden and significant change, the InC-Fuzzy algorithm shows its advantage. In a scenario where irradiation jumps from 500 W/m² to 800 W/m² at 0.6 seconds and then drops to 400 W/m² at 1.2 seconds (lasting for a total of 2 seconds), the total power generated by the PV system using the InC-Fuzzy algorithm reaches 54.03 watts. This represents a 1.69% increase in power compared to the conventional Incremental Conductance algorithm. In simpler terms, the InC-Fuzzy algorithm excels in both stable and rapidly changing irradiation conditions, offering superior power harvesting compared to the conventional approach.

REFERENCES

[1] M. N. HABIBI, D. N. PRAKOSO, N. A. WINDARKO, and A. TJAHJONO, "Perbaikan MPPT Incremental Conductance menggunakan ANN pada Berbayang Sebagian dengan Hubungan Paralel," *ELKOMIKA J. Tek. Energi Elektr. Tek. Telekomun. Tek. Elektron.*, vol. 8, no. 3, p. 546, 2020, doi: 10.26760/elkomika.v8i3.546.

[2] D. Juniyanto, T. Andrasto, and S. Suryono, "Optimalisasi Stand-Alone Photovoltaic System dengan Implementasi Algoritma P&O-Fuzzy MPPT," *J. Tek. Elektro*, vol. 10, no. 1, pp. 1–10, 2018, doi: 10.15294/jte.v10i1.14108.

[3] R. M. Hakim, "Desain dan Implementasi MPPT Berbasis Algoritma Modified Incremental Conductance untuk Photovoltaic dengan Perubhan Iradiasi Matahari yang Cepat," Surabaya, 2018.

[4] S. Anitha, C. Vinay Kumar Reddy, G. Balaram, and G. Ranadheer Reddy, "Design of PV Array Using Boost Converter by Incremental Conductance Mppt Power Technique," *IOP Conf. Ser. Mater. Sci. Eng.*, vol. 981, no. 4, 2020, doi: 10.1088/1757-899X/981/4/042075.

[5] P. K. Mishra and P. Tiwari, "Incremental conductance MPPT in grid connected PV system," *Int. J. Eng. Sci. Technol.*, vol. 13, no. 1, pp. 138–145, 2021, doi: 10.4314/ijest.v13i1.21s.

[6] A. Baihaqiy, T. Hardianto, B. S. Kaloko, M. Gozali, and B. Sujanarko, "Rancang Bangun Sepic Converter Untuk Panel Surya Dengan Mppt Inc Sebagai Pengisian Baterai Sepeda Listrik," *J. Arus Elektro Indones.*, vol. 6, no. 2, p. 38, 2020, doi:

10.19184/jaei.v6i2.19642.

[7] D. N. Prakoso, A. Afandi, M. Arrijal, R. Abdurrahman, and N. A. Windarko, "Perbandingan Metode MPPT Incremental Conductance Incremental Resistance dan Hill Climbing dengan PSIM," *Jetri J. Ilm. Tek. Elektro*, vol. 17, no. 2, pp. 175–190, 2020, doi: 10.25105/jetri.v17i2.6076.

[8] M. Ahmad, A. Numan, and D. Mahmood, "A Comparative Study of Perturb and Observe (P&O) and Incremental Conductance (INC) PV MPPT Techniques at Different Radiation and Temperature Conditions," *Eng. Technol. J.*, vol. 40, no. 2, pp. 376–385, 2022, doi: 10.30684/etj.v40i2.2189.

[9] T. A. Zulhelmi, "Comparisonal Analysis Of Incremental Conductance And Perturb And Observe Methods As MPPT Algorithm In Photovoltaic System," *J. Mekintek J. Mek. Energi, Ind. Dan Teknol.*, vol. 12, no. 1, pp. 17–22, 2021, doi: 10.35335/mekintek.v12i1.23.

[10] L. Shengqing, L. Fujun, Z. Jian, C. Wen, and Z. Donghui, "An improved MPPT control strategy based on incremental conductance method," *Soft Comput.*, vol. 24, no. 8, pp. 6039–6046, 2020, doi: 10.1007/s00500-020-04723-z.

[11] G. H. N. Aldiantama, "Perancangan MPPT Modified Incremental Conductance menggunakan Interleaved Boost Converter untuk Reduksi Osilasi," *J. Tek. Energi Elektr. Tek. Telekomun. Tek. Elektron.*, vol. 10, no. 1, pp. 76–89, 2022.

[12] I. Owusu-Nyarko, M. A. Elgenedy, I. Abdelsalam, and K. H. Ahmed, "Modified variable step-size incremental conductance mppt technique for photovoltaic systems," *Electron.*, vol. 10, no. 19, 2021, doi: 10.3390/electronics10192331.

[13] J. A. Hamonangan, "Review Perbandingan Teknik Maximum Power Point Tracker (MPPT) untuk Sistem Pengisian Daya menggunakan Sel Surya," *J. Teknol. Dirgant.*, vol. 16, no. 2, p. 111, 2019, doi: 10.30536/j.jtd.2018.v16.a2998.

[14] M. S. Al-mohamade and H. D. Al-majali, "Comparison between Fuzzy-logic MPPT and the Exciting Incremental Conductance Method under Fast Varying of Irradiance 2 . Photovoltaic Module Modeling," 2021.

[15] A. Bharathi Sankar Ammaiyappan and R. Seyezhai, "Implementation of fuzzy logic control based mppt for photovoltaic system with silicon carbide (Sic) boost dc-dc converter," *WSEAS Trans. Syst. Control*, vol. 16, pp. 198–215, 2021, doi: 10.37394/23203.2021.16.17.

[16] W. S. E. Abdellatif, M. S. Mohamed, S. Barakat, and A. Brisha, "A fuzzy logic controller based mppt technique for photovoltaic generation system," *Int. J. Electr. Eng. Informatics*, vol. 13, no. 2, pp. 394–417, 2021, doi: 10.15676/ijeei.2020.13.2.9.

[17] K. Loukil, H. Abbes, H. Abid, M. Abid, and A. Toumi, "Design and implementation of reconfigurable MPPT fuzzy controller for photovoltaic systems," *Ain Shams Eng. J.*, vol. 11, no. 2, pp. 319–328, 2020, doi: 10.1016/j.asej.2019.10.002.

[18] M. Merchaoui, M. Hamouda, A. Sakly, and M. F. Mimouni, "Fuzzy logic adaptive particle swarm optimisation based MPPT controller for photovoltaic systems," *IET Renew. Power Gener.*, vol. 14, no. 15, pp. 2933–2945, 2020, doi: 10.1049/iet-rpg.2019.1207.

[19] W. Hayder, E. Ogliari, A. Dolara, A. Abid, M. Ben Hamed, and L. Sbita, "Improved PSO: A comparative study in MPPT algorithm for PV system control under partial shading conditions," *Energies*, vol. 13, no. 8, 2020, doi: 10.3390/en13082035.

[20] E. S. Wirateruna, A. Fitri, and A. Millenia, "Design of MPPT PV using Particle Swarm Optimization Algorithm under Partial Shading Condition," vol. 4, no. 1, pp. 24–30, 2022, [Online]. Available: http://dx.doi.org/10.25139/ijair.v4i1.4327.

[21] D. A. Asoh, B. D. Noumsi, and E. N. Mbinkar, "Maximum Power Point Tracking Using the Incremental Conductance Algorithm for PV Systems Operating in Rapidly Changing Environmental Conditions," *Smart Grid Renew. Energy*, vol. 13, no. 05, pp. 89–108, 2022, doi: 10.4236/sgre.2022.135006.

[22] H. Othmani, D. Mezghani, A. Belaid, and A. Mami, "New approach of incremental conductance algorithm for maximum power point tracking based on fuzzy logic," *Int. J. Grid Distrib. Comput.*, vol. 9, no. 7, pp. 121–132, 2016, doi: 10.14257/ijgdc.2016.9.7.13.

[23] H. Deboucha and S. L. Belaid, "Improved incremental conductance maximum power point tracking algorithm using fuzzy logic controller for photovoltaic system," *Rev. Roum. des Sci. Tech. Ser. Electrotech. Energ.*, vol. 62, no. 4, pp. 381–387, 2017.

[24] R. Fibrianti, "Rancang Bangun SEPIC (Single-Ended Primary Inductance Converter) untuk Aplikasi MPPT (Maximum Power Point Tracker) Jenis Constant Voltage (CV)," *J. Teknol. Elekterika*, vol. 17, no. 2, pp. 7–13, 2020, [Online]. Available: http://jurnal.poliupg.ac.id/index.php/JTE/article/view/2159.

[25] Y. M. Kolewora, E. Firmansyah, and Suharyanto, "Mppt Berdasarkan Algoritma P&O Dan Ic Pada Interleaved-Flyback 250W," *Telematika*, vol. 11, no. 1, p. 18, 2018, doi: 10.35671/telematika.v11i1.603.

[26] I Sutrisno, MA Jami'in, J Hu, MH Marhaban, N Mariun, "Nonlinear Model-Predictive Control Based on Quasi-ARX Radial-Basis Function-Neural-Network", 2014 8th Asia Modelling Symposium, http://repository.ppns.ac.id/1402/1/2014%20AMS.pdf

[27] I. Sutrisno, M. Firmansyah, R. B. Widodo, A. Ardiansyah, M. B. Rahmat, A. Syahid, C. R. Handoko, A. D. Santoso, A.W. B. Santosa, R. Rulaningtyas, E. Setiawan, E. P. Hidayat, D. Wiratno,"Implementation of Backpropagation Neural Network and Extreme Learning Machine of pH Neutralization Prototype", Journal of Physics: Conference Series, https://iopscience.iop.org/article/10.1088/1742-6596/1196/1/012048/pdf